

# Exploring the Higgs Potential Structure with Longitudinally Polarized Vector Bosons

Shikhar Misra

smisra@students.hackleyschool.org

## ABSTRACT

The Higgs boson is crucial to the Standard Model (SM) of particle physics, explaining how fundamental particles receive mass through interactions with the Higgs field. The symmetry breaking mechanism within the Higgs potential, which gives mass to the weak force bosons, is crucial to understanding our universe's structure. However, limitations remain: classifying Higgs-related events and identifying Beyond Standard Model Physics (BSM) signals. Longitudinally polarized vector bosons are sensitive to BSM physics due to their energy-growing behavior in scattering. Yet, processes like  $pp \rightarrow H + Z_L Z_L + jj$  ( $V_L V_L$ ,  $V = W^{\pm}$  or  $Z$ ) remain underexplored due to small cross sections. This study explores modifying Higgs self, vector boson, and double vector boson coupling parameters ( $C3$ ,  $CV$ , and  $C2V$ ) in  $pp \rightarrow H + Z_L Z_L + jj$ , using both on-shell and off-shell Higgs bosons. The goal was to identify variables and coupling strengths that classify Higgs-related events. Monte-Carlo and detection simulations were done using MadGraph, Pythia, and Delphes. Events were filtered for Higgs-related phenomena, and high signal-to-background (S/B) highlighted discriminating variables across modified coupling strengths. Normalized plots revealed leptonic angular,  $b$ -jet distance, and diboson distance variables as the most discriminatory. Raw plots showed  $CV = \pm 2$  and  $C2V = \pm 10$  as key discriminators. Despite small cross sections, Raw S/B ratios exceeded 1 with BSM coupling strengths revealing potential for powerful BSM indicators. The findings of this study enhance Higgs coupling understanding, inform event selection criteria, and provide a framework for future collider experiments to explore the Higgs potential.

## INTRODUCTION

On July 4th, 2012, physicists at CERN revealed that they had discovered a particle that behaves similarly to the theorized Higgs boson (The CMS Collaboration, 2013); a particle which was predicted by Peter Higgs and his team in the Theory of 1964 (Higgs, 1964). The discovery was made through high-energy proton collisions at the Large Hadron Collider (LHC). By observing various decay channels of this new particle and separating its signal from background processes that could mimic Higgs decay, researchers confirmed the existence of the Higgs boson. The Higgs boson is crucial to the Standard Model (SM) of particle physics; it explains how fundamental particles acquire mass through interactions with the Higgs field (Carena, 2023). It also interacts with its own field and has a measured mass of approximately  $125.11 \pm 0.11$  GeV (The ATLAS Collaboration, 2024).

January 2026

Vol 3, No 1.

The perturbative expansion (Fig. 1) of the Higgs potential function,  $V(\phi)$ , which describes interactions with the Higgs field( $\phi$ ), is given as:

$$V(\phi) = \mu^2 \cdot \phi^\dagger \cdot \phi + \lambda \cdot (\phi^\dagger \cdot \phi)^2$$

Where  $\lambda$  is the Higgs coupling constant and  $\mu^2$  is a mass parameter (The University of Edinburgh). If  $\mu^2 > 0$ , the minimum of  $V(\phi)$  is at  $\phi = 0$ , meaning that the Higgs field acquires a vacuum expectation value ( $v$ ) of 0. If  $v = 0$ , then fundamental particles such as the weak force vector ( $W^{+-}$  and  $Z$ ) bosons would be massless.

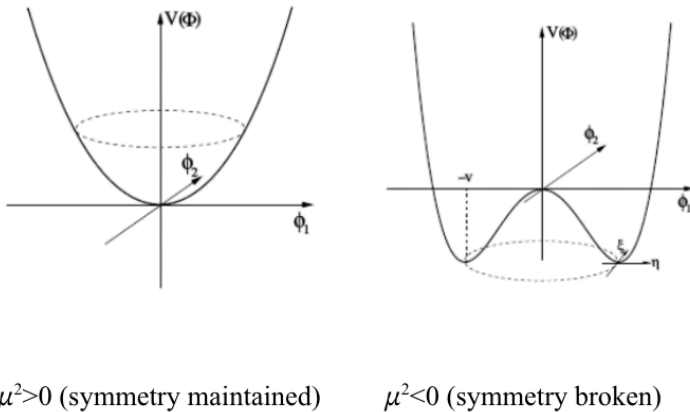


Figure 1: The Higgs Potential Field

Both broken and unbroken symmetries are depicted. Imagine placing a ball along the curve; wherever it settles is where the vacuum expectation value occurs.

This is not what is observed in nature. The weak force carriers gain mass through interactions with the Higgs field, leading to the breaking of weak symmetry (Sutton, 2006):

$$m_{w^{+-}} = \frac{1}{2} \cdot v \cdot g$$

$$m_z = \frac{1}{2} \cdot v \cdot \sqrt{(g^2 + g'^2)}$$

Therefore,  $\mu^2 < 0$ , and  $v \neq 0$  must be true, and symmetry is broken spontaneously. This symmetry breaking is a foundational mystery of our universe and is crucial in explaining why fundamental particles receive mass.

The next step for future Higgs research is to obtain precise measurements of the Higgs coupling. In the electroweak theory, the Higgs boson is coupled to the  $W^\pm$  and  $Z$  bosons and is related to their mass as its square root is inversely proportional to the vacuum expectation value:

$$v = \frac{|H|}{\sqrt{\lambda}}$$

More accurate measurements on the Higgs coupling could help us understand why the electroweak symmetry is broken. Deviations from the SM prediction of the Higgs potential could reveal new physics Beyond the Standard Model (BSM) and enhance our understanding of the foundational laws of the universe (Ellis, 2023).

Francheschini et al. (2018) dubbed a new set of indirect physics effects “High Energy Primary” (HEPs). These effects were probed through longitudinally polarized diboson channels, in particular the  $WZ$  channel. HEP parameters describe BSM effects that grow quadratically ( $E^2$ ) and interfere with SM measurements. These effects are inclusive to all diboson decay channels. The Goldstone Equivalence Theorem tells us that longitudinally polarized vector bosons are connected with the Higgs potential at high energies. The cross section is directly proportional to energy, so as energy increases, the cross section does as well; this rapidly increases the prominence of longitudinally polarized vector bosons in final states. This rapid growth makes such processes highly sensitive to changes in the Higgs potential. Essentially, the HEP parameters allow small BSM contributions to be amplified in sensitivity, particularly in diboson processes. A novel way to parametrize the Higgs coupling is the Higgs without Higgs (HwH) strategy. Henning et al. (2019) employ a method with an off-shell Higgs boson, meaning it cannot be observed directly because it is a virtual particle. HwH looks at energy-growing processes and explores their sensitivity to modifications of the Higgs coupling. Observing the sensitivity to different Higgs coupling values, this study confirms that measuring an off-shell Higgs is competitive with on-shell measurements (Henning, 2019). Barone et al. (2020) proposed a study -utilizing both the high energy diboson channels that Francheschini et al. (2018) found to be sensitive to BSM effects and the off-shell Higgs boson that Henning et al. found to match the accuracy of an on-shell Higgs boson- to measure the energy growing effects of coupling modifications. Barone et al. (2020) wanted to build on previous work by proposing that on-shell Higgs production would be studied simultaneously with the off-shell Higgs production. The processes exploited in the study would contain longitudinally polarized vector bosons and are probed to measure the Higgs coupling. The Higgs self-coupling would also be probed as it is responsible for stabilizing the Higgs mechanism. The signal process looked at would be:  $pp \rightarrow H + W^+ W^- + jj$ . The final state of this process would be subjected to a multivariate analysis where the signal is discriminated from a background sample. Then sub-processes such as  $gg \rightarrow Z_L Z_L$ , from  $qq \rightarrow ZZ$  would be separated and their sensitivity to different Higgs coupling values can be observed. (Barone, 2020).

Previous studies have not yet employed both an off-shell and on-shell Higgs to allow testing of SM values, while in tandem, be sensitive to new physics. Processes such as  $pp \rightarrow H + Z_L Z_L + jj$  have been underexplored due to their significantly smaller cross section. The cross section makes the process much more difficult to express and identify when compared to background processes. Furthermore, the selection techniques used could be improved by applying more relevant event cuts. The goal of this study is to find a signal-to-background discriminating variables in energy-growing longitudinally polarized vector boson

January 2026

Vol 3. No 1.

processes ( $pp \rightarrow H + V_L V_L + jj$ ) containing both an off-shell and on-shell Higgs boson. Then, through observing the effects on these variables by modifying the Higgs self-coupling and vector boson coupling, discrimination as coupling values change will be probed. This will cause the extent of the SM to be tested while searching for indicators of a BSM presence.

## METHODOLOGY

This study uses a combination of computational frameworks to explore SM and BSM phenomenology and effects, focusing on Higgs interactions. MadGraph 3.4.2 and 3.5.2 allow for the computation of cross sections and the generation of high-energy events at a next-to-leading-order (NLO) accuracy (Alwall, 2014). Its functionality allows for both known and theoretical particle interactions. Incorporated with MadGraph is Pythia8, a Monte Carlo-based simulation framework that allows for the description of high-energy collisions, including decay states and initial- and final-state particle showers (Bierlich, 2022). Delphes 3.5.0 was used in combination with MadGraph as well. Delphes is a fast detector simulation tool and it provides an approximate detector response to the events generated by MadGraph and Pythia8 (de Favereau, 2014).

This study focuses on vector boson processes to investigate the Higgs vector boson coupling. Both signal and background vector boson processes were generated through MadGraph. The signal processes were :  $pp \rightarrow H + Z_L Z_L + jj$  (Fig. 2), and the background processes were:  $pp \rightarrow ZZ + jj$ ,  $pp \rightarrow tt + jj$ ,  $pp \rightarrow \ell^+ \ell^- + jj$ , and  $pp \rightarrow W^+ W^- + jj$ . The ZZ system in the signal process has different modes of longitudinal and transverse combinations (longitudinal-longitudinal, transverse-transverse, or transverse-longitudinal). While the signal process is generated inclusively, this process was emphasized because of the BSM sensitivity of the longitudinal-longitudinal mode. The Higgs boson generated is both off-shell and on-shell, which enables expanded experimentation.

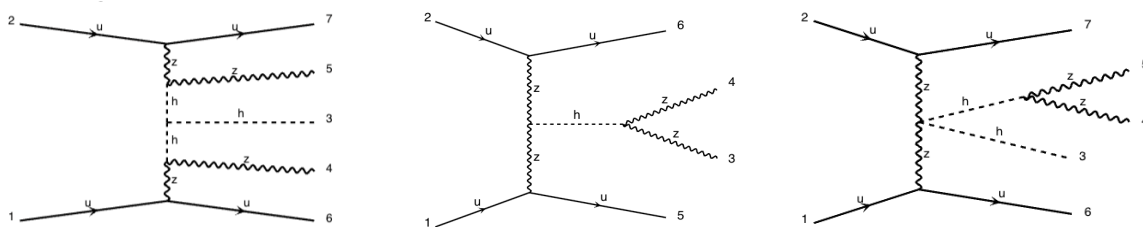


Fig 2. LEFT: Higgs Production Sensitive to C3 Coupling. Internal lines represent off-shell Higgs and external lines represent on-shell Higgs. MIDDLE: Higgs Production and Diboson Decay Sensitive to CV Coupling. RIGHT: Higgs Pair Production and Diboson Decay Sensitive to C2V Coupling.

Only the leptonic decay of vector bosons,  $ZZ \rightarrow 4\ell$ , was considered to reduce background processes. Pythia8 generated the particle shower and Delphes produced an output simulating a detector response. 10,000 events were generated for each signal run and 144,820 events in total for all the background

January 2026

Vol 3. No 1.

processes. Event cut selection was used to filter out irrelevant events (Table 1). Only reconstruction cuts were looked at. Reconstruction cuts are applied after events pass through the detector simulation, rather than ignoring detector response inaccuracy. Filtering out these events refines the dataset by attempting to remove non-Higgs-related events. The  $b$ -jet system is the pair of jets used to reconstruct the  $H \rightarrow bb$  decay. The di-jet system is defined as a pair of jets with VBF (Vector Boson Fusion) or VBS (Vector Boson Scattering) topology. The two highest  $pT$  (transverse momentum) non- $b$  tagged jets are used in the di-jet system.

Table 1: Event Selection Criteria for Reconstruction (Reco) Cuts  
Cuts flow chronologically, top to bottom.

Event Cut flow Parameter:	Value/Description:
$pT^j$ and $\eta_j$	Jet transverse momentum( $pT$ ) > 20 GeV and pseudorapidity( $\eta$ ) < 5
Number of Jets	$\geq 2$ or $\geq 4$ jets found
Di-jet Found	Two jets identified as a di-jet system
$m_{jj}$	Di-jet invariant mass ( $m$ ) > 250 GeV
$pT^\ell$ and $\eta_\ell$	Lepton transverse momentum ( $pT$ ) > 15 GeV and pseudorapidity( $\eta$ ) < 2.5
Number of Leptons	$\geq 2$ or $\geq 4$ leptons found
Opposite-Sign Leptons	$\geq 2$ or $\geq 4$ opposite-sign leptons found
$m_{\nu\nu}$	Vector boson invariant mass ( $m$ ) > 250 GeV or < 150 GeV
$E_T^{miss}$	Missing transverse energy( $E_T^{miss}$ or $MET$ ) of events > 30 GeV or < 30 GeV
Vector Boson System Found	Events with reconstructed vector boson ( $V_L V_L$ ) systems

Once simulation data were generated, the analysis was performed using ROOT 6.32.06. ROOT is an object-oriented programming language developed by CERN. Its application is directed towards particle physics. In this study, ROOT was used for modeling and visualization of data generated by Delphes after event simulation.

The selected events for both the signal and background processes were stored in a ROOT file. These files stored multiple histograms for all the variables measured by Delphes. Combining signal and background plots for a given variable allows for a statistical analysis. The overlaid stacks were assessed on their signal-to-background (S/B) with respect to their “shape”. Variables with high S/B ratios are considered discriminating variables as they allow for improved classification of Higgs events. Before calculating the S/B ratio, every histogram was normalized and scaled to standardize signal-to-background comparisons, allowing both plots to function on the same scale. However, both normalized and unnormalized plots and values were considered. Unnormalized plots give absolute raw sensitivity and reflect the statistical influence of a small cross section of the signal process used. These plots also help understand the efficiency of event selection and cuts. Scaled normalized plots help compare distributions regardless of event count. Normalized plots also emphasize the shape of a given distribution, which highlights discriminatory features such as peaks. The S/B ratio was calculated for bins of every histogram of every variable measured. The benefits of calculated S/B per bin, as opposed to per variable distribution plot, are for the removal of bins with high statistical uncertainty. Statistical uncertainty for Poisson distribution with respect to two functions (signal and background functions, in this case) is given by the formula (*Propagation of Errors—Basic Rules*):

$$\sigma_{x,y}^2 = \left(\frac{\partial f}{\partial x} \cdot \sigma x\right)^2 + \left(\frac{\partial f}{\partial y} \cdot \sigma y\right)^2$$

Because this analysis relies on finite Monte-Carlo simulations, some bins with low occupancy can exhibit inflated S/B values. S/B values with uncertainty greater than 100% were not considered; all decimal places were rounded to three significant figures. If no S/B values passed below 100% uncertainty for a given distribution, the max S/B values are denoted as 0. This filtering is especially relevant in extreme coupling values where event yield is minimized by generator/detector-level effects (e.g., the  $CV \pm 10$  samples, which are discussed in Fig.14).

This methodology was repeated, but further analysis was performed using the Genesis model within MadGraph to explore the effects on particle distributions for modifications of both the Higgs self-coupling (C3), vector boson coupling value (CV), and the double vector boson coupling value (C2V). This signal process was re-run for different values for each coupling (Table 2).

*Table 2: BSM and SM Values of the Higgs self, Vector Boson, and Double Vector Boson Coupling Tested*  
*CV cannot be tested at 0, since all vector boson production methods would be turned off. C2V can be 0, as it only restricts coupling to two vector bosons per interaction.*

Parameter:	Self-Coupling (C3) Strength	Vector Boson Coupling (CV) Strength	Double Vector Boson Coupling (C2V) Strength
Run 1 (All @ SM values):	1(SM)	1(SM)	1(SM)
Run 2-9 (C3 @ BSM values):	-10,-5,-2,-1,0,2,5,10	1(SM)	1(SM)
Run 10- 16 (CV @ BSM values):	1(SM)	-10,-5,-2,-1,2,5,10	1(SM)
Run 17-24 (C2V @ BSM values):	1(SM)	1(SM)	-10,-5,-2,-1,0,2,5,10

While one coupling was being modified, the other two remained at the SM value of 1. Modifications of these values influence decay paths and particle interactions. Through simulating both SM and BSM scenarios, the behavior of Higgs-related events was observed. S/B ratios were calculated for each time the coupling was modified. All variables for each coupling parameter (C3, CV, and C2V) were associated with the highest S/B ratio from within each coupling value. Through this, it can be seen within a given coupling parameter, which coupling strength gives discrimination. Discriminating variables were assessed with different self and vector coupling values alongside the default SM coupling values.

## RESULTS

The purpose of this study was to explore how modifications to the Higgs self, vector boson, and double vector boson coupling parameters influence interactions in longitudinally polarized vector boson processes with the aim of testing the SM and probing BSM physics. This was done through high-energy Monte-Carlo simulations. Then, discriminating variables were identified while observing how S/B ratios change under different coupling strengths. When there was clear discrimination within the normalized plots, it tended to be a function of individual detector-measured variables, while discrimination in raw plots was a function of coupling strength.

Within the S/B heatmaps that follow, each cell reports the maximum S/B value per bin for a given variable/observable (row) at a set coupling value (column). A max S/B value of 0 denotes no values fell under 100% statistical uncertainty. Darker cells indicate higher relative S/B values, so trends and key variables can be observed. Heatmaps, for aesthetics, were split into three categories: Lepton (green to blue), ZZ (salmon to black), and  $bb + jj + MET$  (peach to purple) variables.

Looking at normalized leptonic variables- across C3, CV, and C2V- angular variables, particularly  $\Delta\phi_{\ell 1/2}$  and  $\Delta\phi_{\ell 3/4}$ , stood out as strong discriminators (Fig. 3 and Fig. 4).

January 2026

Vol 3. No 1.

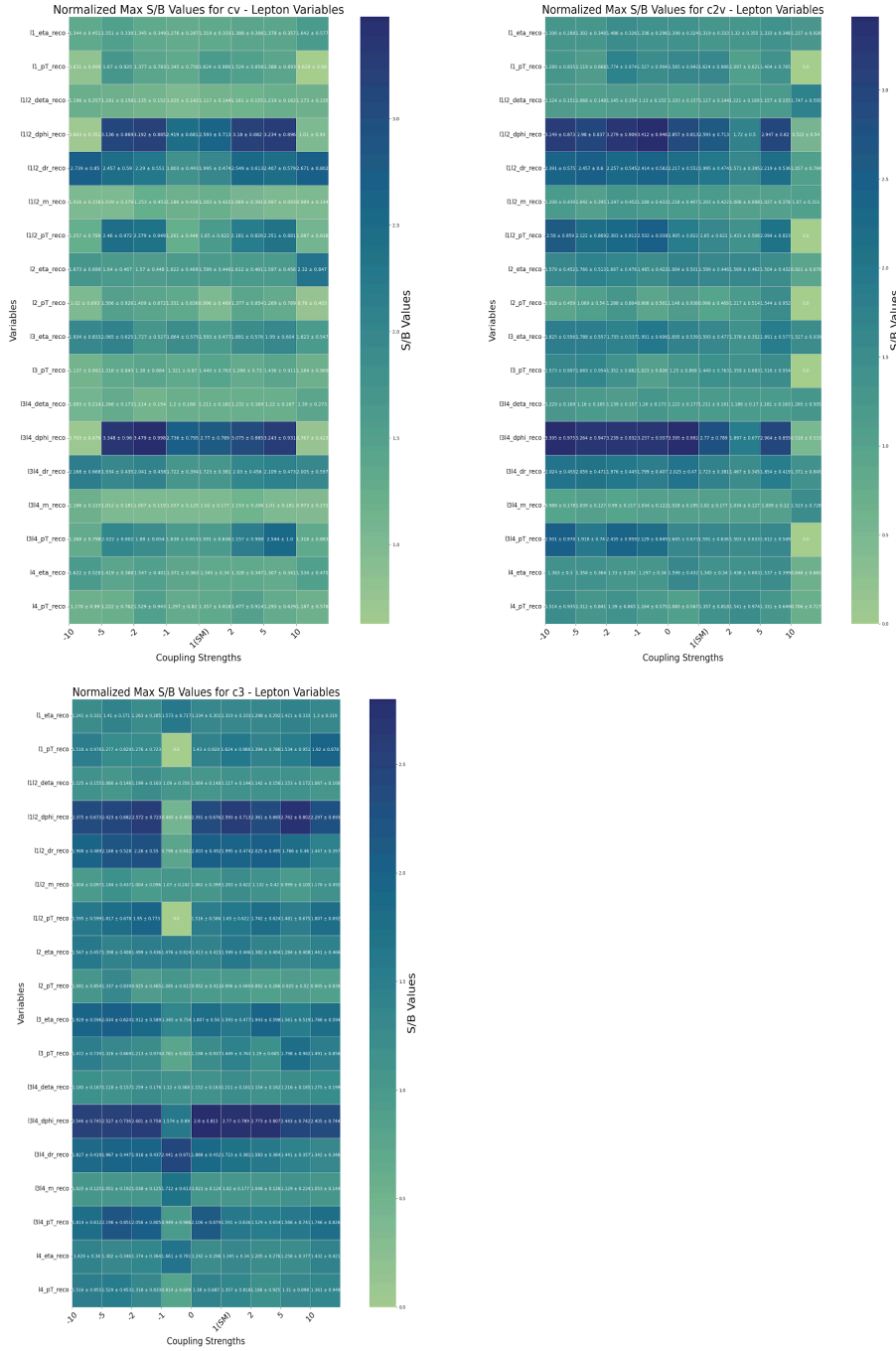


Figure 3. TOP LEFT: Normalized Max S/B Values for CV -Leptonic Variables TOP RIGHT: Normalized Max S/B Values for C2V -Leptonic Variables BOTTOM: Normalized Max S/B Values for C3 -Leptonic Variables

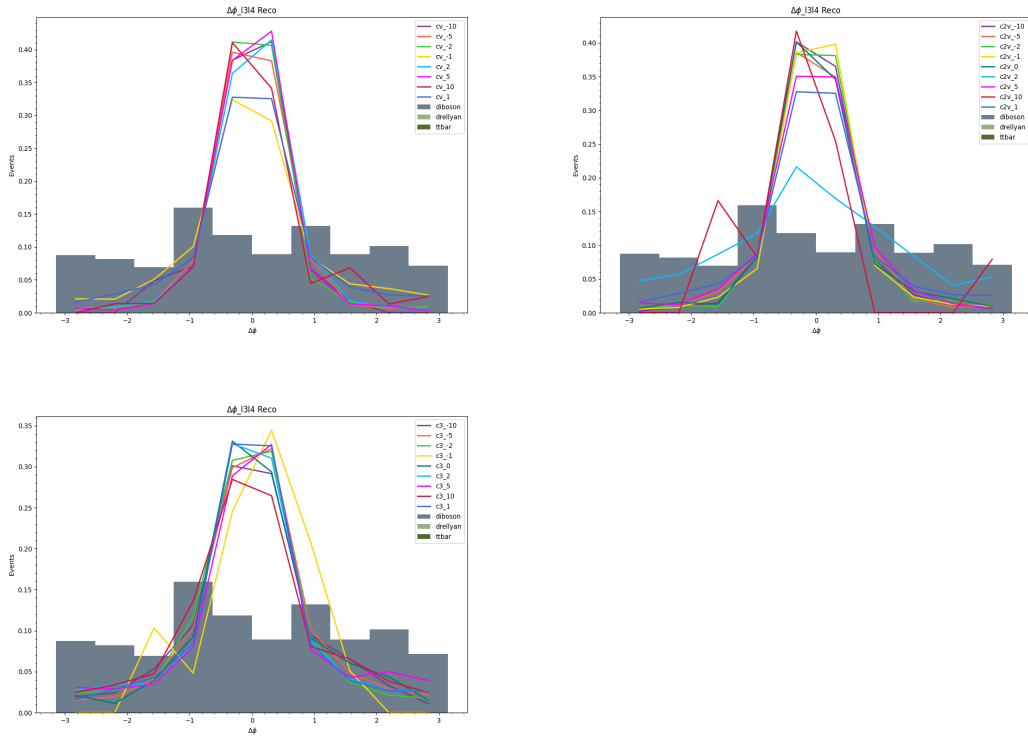


Figure 4. TOP LEFT: Normalized  $\Delta\phi_{\ell 3/4}$  Distribution for CV Modifications TOP RIGHT: Normalized  $\Delta\phi_{\ell 3/4}$  Distribution for C2V Modifications BOTTOM: Normalized  $\Delta\phi_{\ell 3/4}$  Distribution for C3 Modifications

$\Delta\phi_{\ell 3/4}$  notably reached S/B values of  $3.348 \pm 0.96$ ,  $3.479 \pm 0.90$ ,  $3.395 \pm 0.992$ ,  $3.395 \pm 0.975$  and  $2.80 \pm 0.815$  at CV = -5, CV = -2, C2V = 0, C2V = -10 and C3 = 0 respectively. Within the normalized diboson (ZZ) variables,  $\Delta R_{ZZ}$  was a prominent discriminator across all coupling parameters but acted as a greater discriminator within CV and C2V coupling strengths (Fig. 5 and Fig. 6).



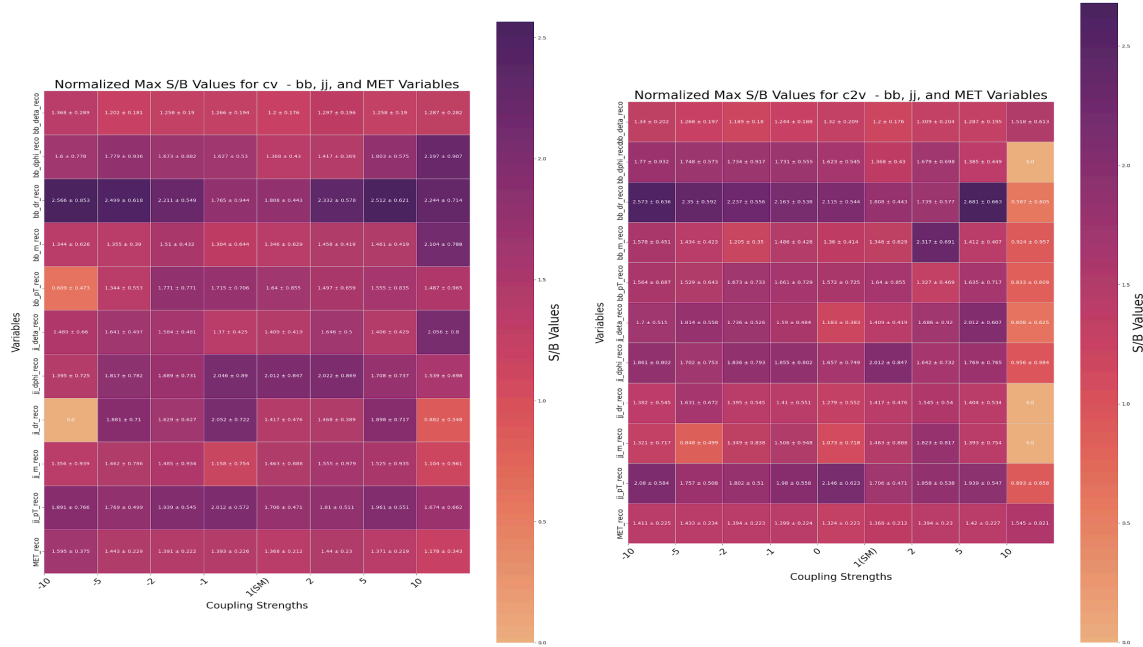


Figure 7. LEFT: Normalized Max S/B Values for CV - b-jet, Di-jet and MET Variables RIGHT: Normalized Max S/B Values for C2V - b-jet, Di-jet and MET Variables

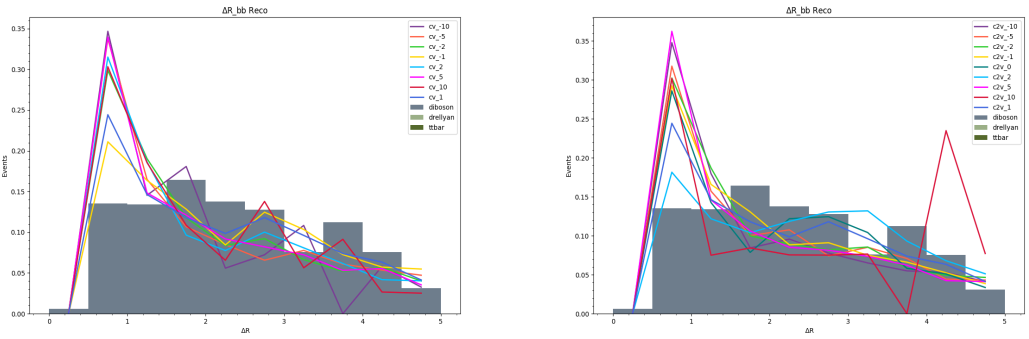


Figure 8. LEFT: Normalized  $\Delta R_{bb}$  Distribution for CV Modifications RIGHT: Normalized  $\Delta R_{bb}$  Distribution for C2V Modifications

$\Delta R_{bb}$  reached S/B values of  $2.681 \pm 0.663$ ,  $2.573 \pm 0.636$ ,  $2.566 \pm 0.853$ , and  $2.512 \pm 0.621$  at C2V = 5, C2V = -10, CV = -10, and CV = 5 respectively. Within the raw S/B values, there wasn't much discrimination across all modifications of the C3 coupling. The highest S/B values achieved was  $0.148 \pm 0.107$  from the  $\Delta R_{t3/4}$  distribution at C3 = -10 (Fig. 9)

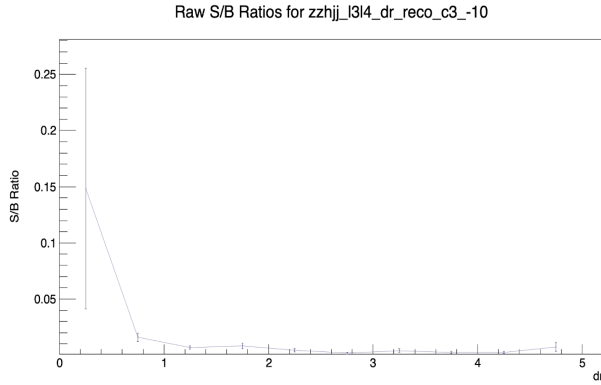


Figure 9: S/B ratios for Raw  $\Delta R_{l3/4}$  Distribution at  $C3 = -10$

This graph is used to highlight the very small range of S/B values, showing that the signal would not be visible compared to the background.

Across all variables: leptonic, diboson,  $b$ -jet, di-jet, and MET, C2V at a strength of  $\pm 10$  and CV at a strength of  $\pm 2$  functioned as the discriminators rather than the individual variables (Fig.10, Fig. 11, and Fig. 12).

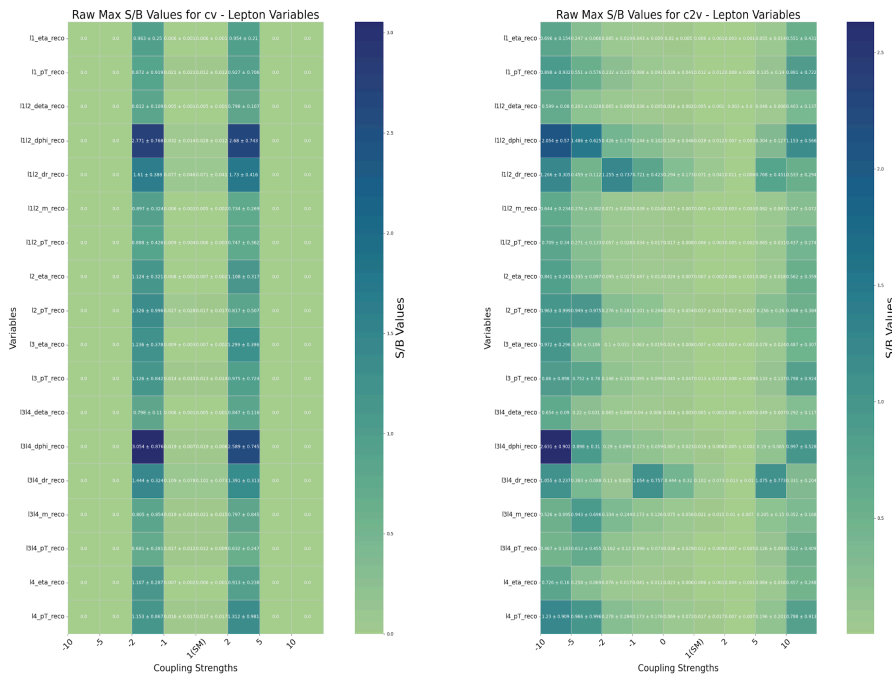


Figure 10. LEFT: Raw Max S/B Values for CV -Leptonic Variables RIGHT: Raw Max S/B Values for C2V -Leptonic Variables

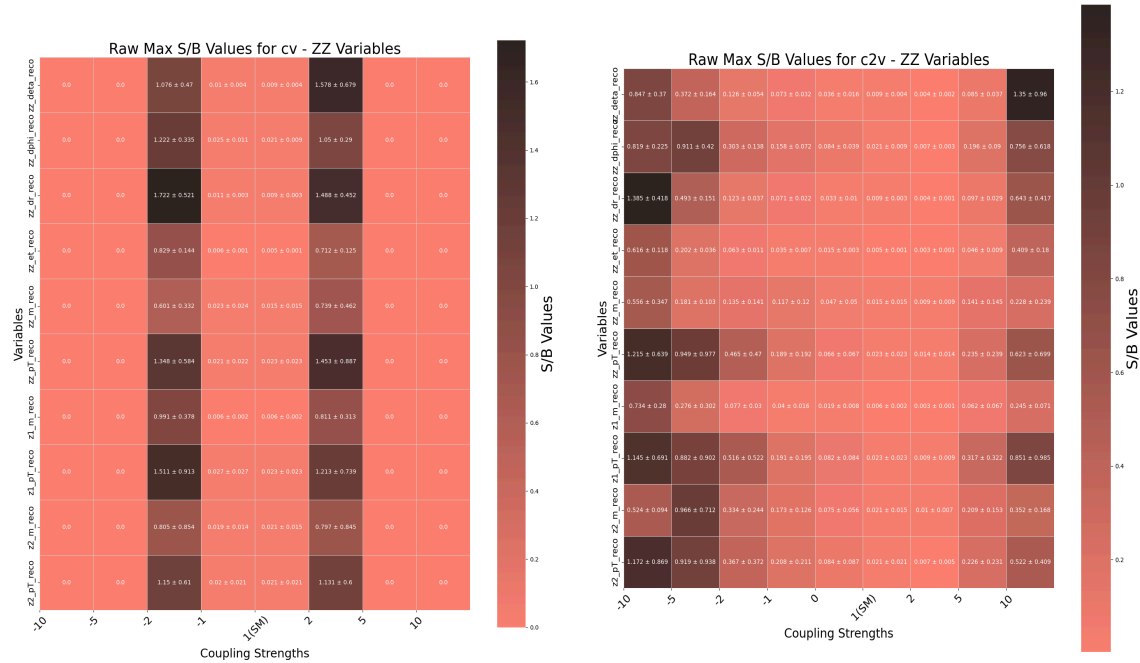


Figure 11. LEFT: Raw Max S/B Values for CV -Diboson Variables RIGHT: Raw Max S/B Values for C2V -Diboson Variables

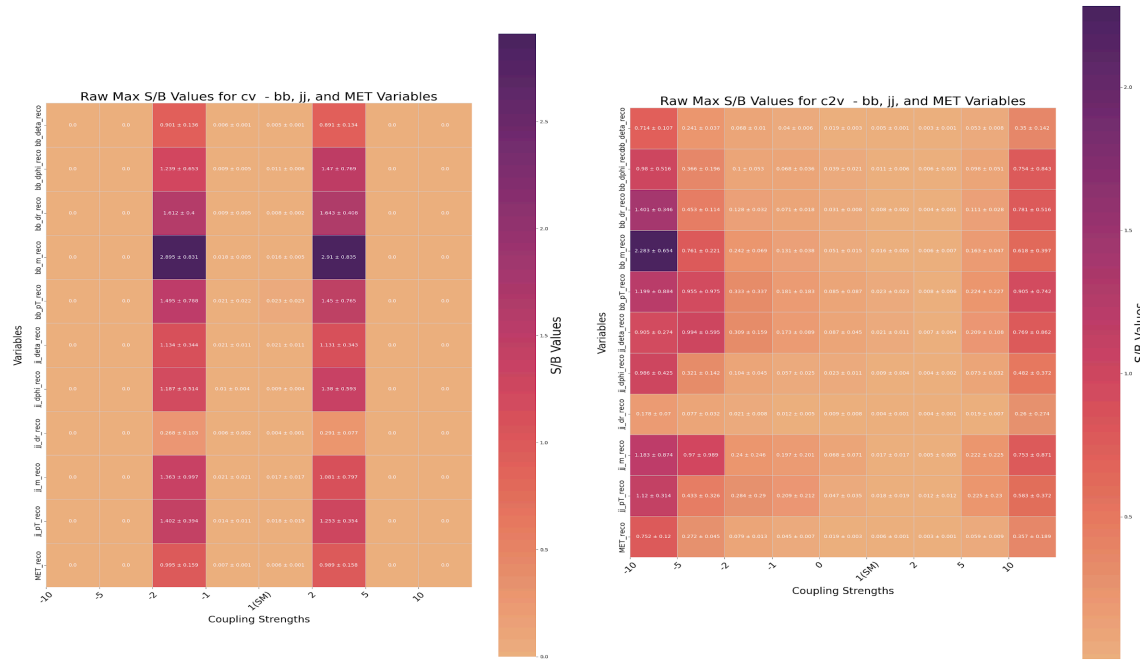


Figure 12. LEFT: Raw Max S/B Values for CV - b-jet, Di-jet and MET Variables RIGHT: Raw Max S/B Values for C2V - b-jet, Di-jet and MET Variables

$C2V = -10$  reached a S/B value of  $2.631 \pm 0.902$  at  $\Delta\phi_{\ell 3/4}$  and  $CV = -2$  reached a S/B value of  $3.054 \pm 0.876$  at  $\Delta\phi_{\ell 3/4}$ .  $M_{bb}$  within  $C2V = -10$  and  $CV \pm 2$  was a strong discriminator (Fig. 13)

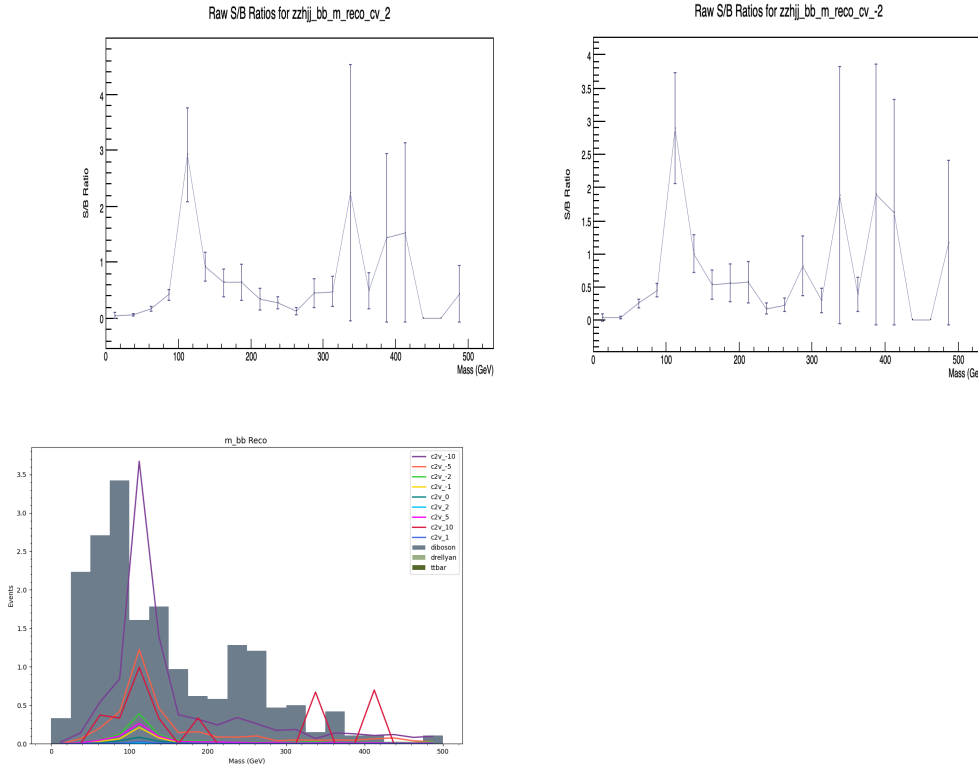


Figure 13. TOP LEFT: S/B ratios for Raw  $M_{bb}$  Distribution at  $CV=2$  TOP RIGHT: S/B ratios for Raw  $M_{bb}$  Distribution at  $CV=2$  BOTTOM: Raw  $M_{bb}$  Distribution for  $C2V$  Modifications

For  $CV = \pm 2$ , a signal-to-background plot could not be shown visually because other  $CV$  strengths with high statistical uncertainty had inflated S/B values and  $CV = \pm 2$  could not be seen in a signal-to-background plot.

$M_{bb}$  accomplished S/B values of  $2.910 \pm 0.835$ ,  $2.895 \pm 0.831$   $2.283 \pm 0.654$  at  $CV = 2$ ,  $CV = -2$ , and  $C2V = -10$  respectively.

## DISCUSSION

In normalized plots, angular variables such as  $\Delta\phi_{\ell 3/4}$  and  $\Delta\phi_{\ell 1/2}$  and distance variables such as  $\Delta R_{ZZ}$  and  $\Delta R_{bb}$  stood out as the strongest discriminating variables. Within the raw plots, modifications to the vector and double vector boson coupling demonstrated sensitivity to BSM effects. The raw plots represented absolute sensitivity and it was not expected for these values to exceed S/B ratios of 1. However, discrimination within  $CV = \pm 2$  and  $C2V = \pm 10$  consistently yielded values above 1. This could either suggest a systematic shift in distributions- from detector sensitivity or event selection criteria- due to the uniformity in discrimination, or it could represent an optimal range where the energy growing effects of longitudinally polarized vector boson interactions become the most pronounced.

January 2026

Vol 3. No 1.

The implications of these results contribute to both the SM and BSM frameworks. The mentioned discriminating variables will aid in identifying Higgs-related events by improving detection sensitivity and highlighting subtle distribution features. The results from modifying coupling values emphasize the efficacy of the analysis structure, particularly event selection criteria. They also act as a powerful indicator of BSM effects and how distributions will change with a BSM presence. Normalized results can be fed into machine learning algorithms to improve the understanding of distribution shapes, thus helping event classification. Raw results can also aid in that respect, but they can be particularly useful as BSM indicators because they represent absolute sensitivity in this process. Integrating this methodology with colliders such as the Large Hadron Collider (LHC) or eventually the High-Luminosity-LHC (HL-LHC) will provide a platform to validate BSM indicators through its improved detector sensitivity, train machine learning models at higher event counts, and help reduce statistical uncertainty. Notably, the HL-LHC will scale the efficacy of this work by offering a greater chance to detect BSM physics. Over its lifetime, the HL-LHC plans to have integrated luminosity ten times what the LHC had. This will greatly increase the event yield for processes with small cross sections, such as  $pp \rightarrow H + ZLZL + jj$ , and thereby enhance the ability to probe BSM physics.

Continuing to refine our understanding of the SM and building our knowledge beyond, will lay the foundation for new physics that addresses the questions surrounding the Higgs mechanism and spontaneous symmetry breaking.

This study faced challenges with certain coupling values:  $CV = \pm 10$ . Delphes configuration issues led to a significantly smaller dataset for those values compared to the rest. This, in turn, contributed to its high statistical uncertainty and inability to be analyzed in terms of S/B values (Fig. 14).

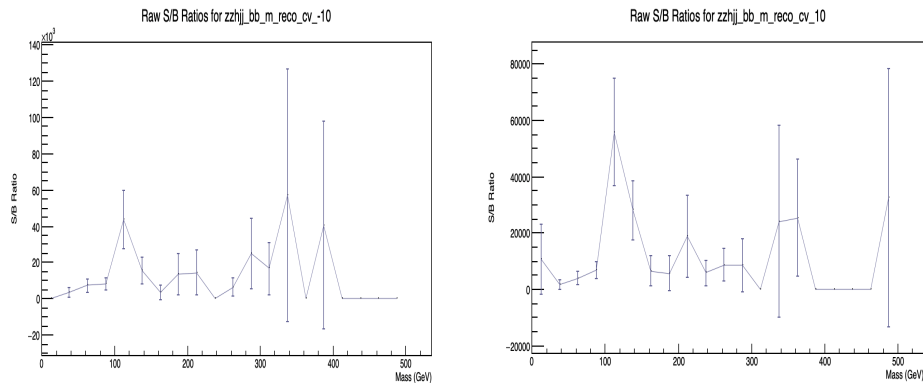


Fig 14. LEFT: S/B ratios for Raw  $M_{bb}$  Distribution at  $CV=-10$  RIGHT: S/B ratios for Raw  $M_{bb}$  Distribution at  $CV=10$

These two S/B distributions are examples of how, in these particular coupling strengths, small event sizes led to improper weighting; this is evident by the y-axis scale.

This methodology can also be run, but instead of two coupling parameters staying at 1 while the third is modified, two or more coupling parameters can be modified simultaneously. This could show how the presence of multiple BSM indicators simultaneously affects distributions. Event selection criteria can be

January 2026

Vol 3. No 1.

further refined to allow for greater discrimination, particularly for modifications within the C3 parameter. The statistical uncertainty cutoff for this experiment was 100%; this was chosen to capture valuable data without it being statistically insignificant. Although further increasing the sample size for each signal run would allow a lower cutoff for uncertainty, coupling strengths with high uncertainty, besides  $CV = \pm 10$ , already had low S/B values; therefore, it is unlikely that anything with statistical significance was missed. While this study was primarily limited by statistical uncertainty, there are several systemic limitations that could shift S/B values and rankings of discriminating variables. In generation, MadGraph inherits theoretical Parton Distribution Functions (PDF), which describe the probability density of finding a parton inside hadrons. This study did not modify the scale (energy level) or PDF shower modeling, which can lead to changes in momentum fractions of quarks/gluons and thus alterations of kinematic observables, such as transverse momentum. Modification to the scale and PDFs also lead to more accurate NLO interaction calculations beyond Quantum Chromodynamics. The fast detection simulator, Delphes, assumes an idealized geometry around the beam axis. This neglects dead material and cracks, leading to potential discrepancies in distance and angular variables. Additionally, expanding the dataset to include the full Z boson decay, not just leptonic decay, would increase the application and understanding of the sensitivity to BSM effects.

## CONCLUSION

This study aimed to explore the Higgs potential structure by observing the effects of modifying the Higgs self-coupling, vector coupling, and double vector coupling parameters. Through processes involving longitudinal vector bosons and both on and off-shell Higgs bosons, the effects of BSM and SM physics were probed. Major results showed that leptonic angular and di-jet and  $b$ -jet distance variables were the greatest discriminators in normalized plots. These variables highlighted how the shapes of their distributions function and change as the coupling strength is altered. Machine learning algorithms can use this data to improve event classification by identifying subtle shifts in distributions. In certain vector coupling values, raw S/B ratio plots demonstrated significant sensitivity to BSM effects in the vector and double vector boson parameters. These parameter strengths achieved S/B values greater than one despite the plots being raw. Achieving these S/B ratios shows the potential for the results to function as strong BSM indicators.

This work serves as a landscape to describe the Higgs potential function by enhancing precision in Higgs coupling measurements. These enhancements can improve sensitivity in LHC or HI-LHC collider experiments in detecting BSM effects. Additionally, the use of an off-shell Higgs boson expanded measurements to include interactions not captured by just an on-shell Higgs; this, combined with longitudinally polarized vector bosons, was validated as a robust probe for BSM effects. Overall, this work provides a strong methodology for testing at colliders and addresses questions about the Higgs mechanism's spontaneous symmetry breaking, testing the extent of our current knowledge while searching for new physics.

## ACKNOWLEDGEMENTS

I would like to thank my mentor, Dr. Gaetano Barone, whose guidance has been invaluable throughout my research process. His patience in explaining complex concepts, receptiveness, and consistent support have not only helped me navigate this study but have also inspired a passion for the work I am doing. Secondly, I would like to thank Doctoral Researcher Spencer Ellis for his technical help and guidance. I also want to extend my gratitude to my Science Research teacher, Dr. Andrew Ying. His support, encouragement, and commitment to fostering my scientific development are something that I am thankful for. Lastly, I would like to thank my parents for providing me with the opportunities and resources I have, for introducing me to the world of science, and for teaching me how to be curious.

## REFERENCES

- Carena, M., Grojean, C., Kado, M., & Sharma, V. (2023, August 23). *II. Status of Higgs Boson Physics*. <https://pdg.lbl.gov/2023/reviews/rpp2022-rev-higgs-boson.pdf>
- Henning, B., Lombardo, D., Riemann, M., & Riva, F. (2019, October 15). *Higgs couplings without the Higgs*. arXiv.org. <https://arxiv.org/abs/1812.09299>
- Barone, G., & Xu, L. (2020, August 30). *Exploring polarized vector bosons to measure the Higgs boson properties in diboson channels*. [https://www.snowmass21.org/docs/files/summaries/EF/SNOWMASS21-EF1\\_EF2-105.pdf](https://www.snowmass21.org/docs/files/summaries/EF/SNOWMASS21-EF1_EF2-105.pdf)
- Ellis, S., Barone, G, Mondal S. (2023). *Unfolding the Higgs potential structure*. CMS at Brown.
- Sutton, C. (2006, July). *Electroweak theory*. Encyclopædia Britannica. <https://www.britannica.com/science/electroweak-theory>
- The ATLAS Collaboration. (2024, January 22). *Combined measurement of the higgs boson mass from the  $H \rightarrow \gamma\gamma$  and  $H \rightarrow ZZ^* \rightarrow 4\ell$  decay channels with the atlas detector using  $\sqrt{s} = 7, 8$  and 13 TEV pp collision data*. arXiv.org. <https://arxiv.org/abs/2308.04775>
- Franceschini, R., Panico, G., Pomarol, A., Riva, F., & Wulzer, A. (2018, June 8). *Electroweak precision tests in high-energy Diboson processes*. arXiv.org. <https://arxiv.org/abs/1712.01310>
- The University of Edinburgh. (n.d.). *Lecture 17 - the higgs boson*. <https://www2.ph.ed.ac.uk/~playfer/PPLect17.pdf>
- University of Washington. (n.d.). *Propagation of errors—basic rules*. [https://courses.washington.edu/phys431/propagation\\_errors\\_UCh.pdf](https://courses.washington.edu/phys431/propagation_errors_UCh.pdf)

January 2026

Vol 3. No 1.

The CMS Collaboration. (2013, January 28). *Observation of a new boson at a mass of 125 GeV with the CMS experiment at the LHC*. arXiv.org. <https://arxiv.org/abs/1207.7235>

Higgs, P. (1964, August 31). *Phys. rev. Lett.* 13, 508 (1964) - *broken symmetries and the masses of gauge bosons*. <https://journals.aps.org/prl/abstract/10.1103/PhysRevLett.13.508>

de Favereau, J., Delaere, C., Demin, P., Giammanco, A., Lemaître, V., Mertens, A., & Selvaggi, M. (2014, March 21). *DELPHES 3, a modular framework for fast simulation of a generic collider experiment*. arXiv.org. <https://arxiv.org/abs/1307.6346>

Bierlich, C., Chakraborty, S., Desai, N., Gellersen, L., Helenius, I., Ilten, P., Lönnblad, L., Mrenna, S., Prestel, S., Preuss, C. T., Sjöstrand, T., Skands, P., Uthmeim, M., & Verheyen, R. (2022, March 22). *A comprehensive guide to the physics and usage of Pythia 8.3*. arXiv.org. <https://arxiv.org/abs/2203.11601>

Alwall, J., Frederix, R., Frixione, S., Hirschi, V., Maltoni, F., Mattelaer, O., Shao, H.-S., Stelzer, T., Torrielli, P., & Zaro, M. (2014, July 21). *The automated computation of tree-level and next-to-leading order differential cross sections, and their matching to Parton shower simulations*. arXiv.org. <https://arxiv.org/abs/1405.0301>

Melo, I. (n.d.). *Higgs potential and fundamental physics*. [https://indico.in2p3.fr/event/19252/contributions/72633/attachments/54437/71264/EWPT\\_Writeup.pdf](https://indico.in2p3.fr/event/19252/contributions/72633/attachments/54437/71264/EWPT_Writeup.pdf)

Plehn, T., & Rauch, M. (2005, July 28). *The quartic higgs coupling at Hadron Colliders*. arXiv.org. <https://arxiv.org/abs/hep-ph/0507321>

Mancini, G. (n.d.). *From the K-framework to the EFT approach for the higgs ...* <https://agenda.infn.it/event/10076/contributions/424/attachments/380/417/gmanciniCosenza.pdf>